PCCP

Accepted Manuscript

ROYAL SOCIETY OF CHEMISTRY

www.rsc.org/pccp

Potential Energy Surface of Fluoroxene: Experiment and Theory

Iciar Uriarte,[a] Patricia Écija,[a] Lorenzo Spada,[a],[b] Eneko Zabalza,[a] Alberto Lesarri,[c] Francisco J. Basterretxea,[a] José A. Fernández,[a] Walther Caminati,[b] and Emilio J. Cocinero[a]*

[a] Departamento de Química Física, Facultad de Ciencia y Tecnología, Universidad del País Vasco (UPV/EHU), Campus de Leioa, Ap. 644, E-48080, Bilbao, Spain.

[b] Department of Chemistry, University of Bologna, Via Selmi 2, 40126, Bologna, Italy.

[c] Departamento de Química Física y Química Inorgánica, Facultad de Ciencias, Universidad de Valladolid, E-47011, Valladolid, Spain.

Corresponding author:

Emilio J. Cocinero
Phone: +34 94 601 5386
E-mail address: emiliojose.cocinero@ehu.es
Web: http://www.grupodeespectroscopia.es/MW

KEYWORDS: Anesthetics, rotational spectroscopy, conformation analysis, substitution structure, supersonic expansion.

Abstract

The potential energy surface (PES) of the general anesthetic fluoroxene (2,2,2-trifluoroethyl vinyl ether) was probed in a supersonic jet expansion using broadband chirped-pulse Fourier transform microwave (CP-FTMW) spectroscopy and theoretical calculations. The PES is dominated by a single conformation, as other stable minima are shown to kinetically relax in the expansion to the global minimum. Consistently, the rotational spectrum reveals a single conformation. Fluoroxene adopts a C_S heavy-atom planar skeleton structure in the gas phase, with a *cis*-*trans* conformation (*cis* for the CH_2=CH-O-CH_2- and *trans* for the =CH-O-CH_2-CF_3 part). The sensitivity of the recently-built CP-FTMW spectrometer at the UPV/EHU is demonstrated by the detection of five isotopologues of fluoroxene in natural abundance, corresponding to the ^{13}C and ^{18}O monosubstituted species. The r_S and r_0 structures were calculated and are in good agreement with theoretical predictions at MP2, B3LYP and M06-2X methods.

Introduction

General anesthetics play a key role in modern medicine and are widely used inhalational and intravenously in nowadays surgical operations. Despite the common use of these drugs, the details of their mechanism of action are still subject to debate. This controversy is fueled by the large variety of substances that can work as anesthetics, having different shapes, sizes and a large diversity of functional groups in their structures (i.e. di- or triatomic gases, ethers, alcohols, haloalkanes, etc). Some of these general anesthetics (such as propofol) seem to work through an interaction with ligand-gated ion channels which would inhibit neuronal synapses.[1,2] However, this cannot be extended to all general anesthetics and further studies about their mechanism of action are needed. Understanding of the structure and conformation of anesthetics as well as their preferences for specific intermolecular interactions may provide insight into the modeling of binding sites and docking mechanisms at the protein active sites.

In this sense, the gas phase provides a unique scenario to investigate the intrinsic molecular properties of anesthetics and their intermolecular binding forces. The lack of interferences from solvent interactions or crystal packing effects makes it possible to study the molecule under isolation conditions and gives access to its conformation and structure in the absence of “external” interactions. Moreover, the use of supersonic expansions allows one to isolate weakly-bound intermolecular complexes and, thus, the study of the intermolecular interactions that govern the binding preferences of the anesthetics.

Several spectroscopic techniques have been applied in the gas phase to the structural study of general anesthetics. Mass-resolved laser electronic spectroscopy has been used for the study of species such as propofol[3] and benzocaine,[4] for which several intermolecular complexes and clusters have been analyzed in supersonic expansions.[5,6] This kind of electronic spectroscopy techniques allows one to study moderate-large size molecular systems in the gas phase (peptides,[7,8,9,10] carbohydrates,[11,12,13,14] nucleobase pairs,[15,16,17] etc) but they require in most of the cases a chromophore and the conformational assignment is not always unambiguous.

On the other side, microwave spectroscopy provides the most accurate structural description of molecular systems of small-medium size in the gas phase. Their inherent resolution (sub-Doppler) allows one to unambiguously identify conformers,[18] tautomers,[19] isotopologues[20] and enantiomers[21] as independent species. In addition, the validity of theoretical quantum chemistry methods can be evaluated. The conformational landscape of these molecules and their related intermolecular complexes can be extensively investigated, since the different conformations can be clearly distinguished in the rotational spectrum. In the last decades, most of the microwave spectrometers have been based on the original design by Balle and Flygare (Fourier transform microwave, FTMW).[22] For example, the structural properties of the anesthetics sevoflurane[23] and isoflurane[24] were investigated in such spectrometers. The isoflurane-water complex[25] was also studied using FTMW spectroscopy in order to assess the effect of microsolvation on the conformational landscape of the anesthetic. In 2005, Pate introduced a new design for a microwave spectrometer based on chirped pulse (CP) microwave excitation (CP-FTMW).[26] This design overcomes the problem of the narrow bandwidth of conventional FTMW spectrometers and reduces significantly the spectral acquisition time. Thanks to this new instrument, the anesthetic propofol,[27] the sevoflurane dimer[28] and the sevoflurane-benzene complex[29] could be studied in a supersonic expansion; the latter study provides some insights into the molecular recognition properties of this anesthetic.

Fluoroxene (2,2,2-trifluoroethyl vinyl ether, Scheme 1) exhibits general anesthetic properties and was used as an inhalational anesthetic. In the 1970s, it was removed from the market because of its flammability and toxicity. No further studies were performed to elucidate its mechanism of action, which remains unclear. In 1974, an infrared spectroscopic analysis in the vapor state[30] indicated that the skeleton of the molecule adopts a planar conformation although it was not possible to determine the specific configuration of the vinyl (CH_2=CH-O-CH_2-) and the trifluoroethoxy (=CH-O-CH_2-CF_3) groups (Figure 1). A low resolution microwave (LRMW) rotational study in 1975[31] suggested a vinyl *cis* – trifluoroethoxy *trans* (*cis*-*trans*) planar conformation for fluoroxene in the gas phase, discarding any vinyl *trans* structure. An analysis of the Q branch band head of several μ_b transitions in the LRMW spectrum[32] was later found consistent with vinyl *cis* conformations but was unable to conclude about the *trans* or *gauche* conformations for the trifluorethoxy group. None of these studies was conclusive so the conformation of fluoroxene has remained unclear so far.

The aim of the present work is to carry out an exhaustive exploration of the potential energy surface (PES) of fluoroxene and to unambiguously determine its conformation and structure in the gas phase by means of high resolution rotational spectroscopy in a supersonic expansion. The combination of both techniques allows studying the isolated molecule and the assessment of its intrinsic conformational and structural preferences.

Experimental and computational methods

The rotational spectrum of fluoroxene was measured in a recently built CP-FTMW spectrometer at the University of the Basque Country (UPV/EHU). This instrument is based on the original Pate's design[26] and allows acquiring the rotational spectra in the 7.0-18 GHz frequency range in a single molecular pulse. Briefly, a 1 μs chirped pulse was generated in an Arbitrary Waveform Generator, covering 11 GHz. This broadband pulse was frequency-upconverted with a broadband mixer and amplified in a travelling wave tube amplifier (250 W). It was later broadcast inside a high vacuum chamber (evacuable down to 10^{-6} mbar) by using a horn antenna. The excitation induces a polarization, resulting in a spontaneous molecular emission signal. This emission was collected with the aid of a second horn antenna and sent to a digital oscilloscope with 20 GHz bandwidth. For each chirped pulse, a 20 μs time domain signal was recorded in the scope. In the current set-up, 10 chirped pulses were used in each molecular pulse.

A commercial sample of fluoroxene (97%) was used without any further purification. The anesthetic is a very volatile liquid (vapour pressure of 381 mbar at 20ºC) with a low boiling point (43 ºC). The sample was prepared as a gas mixture of about 0.5% of fluoroxene in Ne:He (80:20) and was expanded into the spectrometer vacuum chamber at a stagnation pressure of ~ 2 bar.

Theoretical calculations supplemented the experimental work. First, a conformational search was accomplished using a fast molecular mechanics method (Merck Molecular Force Field: MMFFs[33]). Advanced Monte Carlo and large-scale low-mode conformational search algorithms were used to scan the conformational landscape of fluoroxene. Then, all structures within the 0-20 kJ mol^{-1} energy window were fully reoptimized using quantum chemical calculations. We compared the predictive capabilities of several molecular orbital methods, in particular *ab initio* (MP2) and density functional theory (B3LYP and M06-2X) models. In all cases a Pople's triple-ζ 6-311++G(d,p) basis set was used, as implemented in the Gaussian 09 software package.[34] Relative energies, rotational and centrifugal distortion constants and dipole moments of the lowest lying conformers were predicted. In addition, the PES was evaluated with a grid of 169 calculations at MP2/6-311++G(d,p), varying the torsion angles C_1-C_2-O_3-C_4 and C_2-O_3-C_4-C_5 with a 15º step. Finally, we also estimated the isomerization barriers between different conformers at intervals of 10º at MP2/6-311++G(d,p).

Results

-Theoretical calculations

MP2, M06-2X and B3LYP methods predict that the conformational landscape of fluoroxene in the 0-20 kJ mol^{-1} range exhibits the four minima of Figure 1. A bidimensional PES was created using the torsion angles C_1-C_2-O_3-C_4 and C_2-O_3-C_4-C_5, which were scanned every 15 degrees. All calculations agree that the C_S-symmetry *cis-trans* conformer is by far the most stable and is presumed to dominate the experimental rotational spectrum. The *cis-gauche* conformation suggested in previous works is predicted at an electronic energy of 7.3 kJ mol^{-1} (MP2). The *trans-gauche* and *trans-trans* structures are predicted at electronic energies of 7.5-9.6 kJ.mol^{-1} (MP2). The dihedral angles of the three higher energy conformers show some distortion from the tetrahedral structure due to the fluorine atoms. The most relevant predicted spectroscopic parameters of the four conformers are shown in Table 1.

-Rotational spectrum

An overview of the experimental spectrum of fluoroxene in the 6.0-18 GHz region is presented in Figure 2 alongside the MP2 predicted spectra of the lowest-lying conformers. The experimental spectrum is the average of 1,675,600 accumulated spectra after an acquisition time of nearly 48 hours. The spectrum is very congested, consisting of nearly 2200 lines with a signal-to-noise ratio (SNR) $\geq$ 3/1. Visual inspection suggests that it is dominated by the most stable *cis-trans* species. A total of 190 rotational transitions were fitted to a semirigid asymmetric rotor Hamiltonian in the Watson S-reduction.[35] The most intense transition in the assignment ($J_{K-1,K+1}=4_{1,3} \leftarrow 3_{1,2}$) had a SNR ≈ 13000/1. A preliminary assignment with a set of 26 ^{a}R transitions yielded precise values of B and C rotational constants. A subsequent assignment of 43 μ_b transitions allowed the A rotational constant to be fitted. This permitted the assignment of further transitions, including ^aR, ^aQ, ^bR, ^bQ and ^bP branch lines. The determined rotational and centrifugal distortion constants are summarized in Table 2 alongside the LRMW constants.[32] Comparison between theory (Table 1) and experiment (Table 2) seems to indicate that the observed species is the *cis-trans* conformation of fluoroxene. Table 2 also displays the values of the rotational constants estimated in the LRMW study by Dennison et al.[32] with discrepancies >10 MHz for the three rotational constants. The present study clearly improves the accuracy of the previous results. Relative errors are in the 0.5-0.9%, 0.4-1.6% and 0.2-1.5% ranges for A, B and C respectively depending on the theoretical method. The predicted rotational constants correspond to the equilibrium structure. The largest errors are due to the B3LYP calculations, while M06-2X provides the most accurate data. The full list of rotational transitions observed for the parent species is given as Supporting Information in Table S1. Comparison between the original spectrum and the result of removing the lines assigned to the parent species of fluoroxene is depicted in Figure 3, showing that the spectrum is clearly dominated by the *cis-trans* conformer. However, the zoom presented in Figure 3 shows that a large number of weaker lines (ca. 15 times weaker than the most intense transition of the *cis-trans* conformer) still remain unassigned.

-Isotopic species and structure

Once the transitions assigned to the parent species were discarded, a set of approximately 2000 weaker lines (with a SNR ≥ 3/1) remained in the spectrum. Among these, a total of 354 transitions were assigned to the ^{13}C (natural abundance ~ 1.1%) and ^{18}O (~0.2%) monosubstituted isotopologues of fluoroxene. Several μ_a and μ_b transitions of the four singly substituted ^{13}C species and the ^{18}O species could be fitted following the same procedure as in the parent species. Figure 4 displays the region of the spectrum with the assignment of the $4_{0,4} \leftarrow 3_{0,3}$ transition for the five monosubstituted species. All the transitions assigned to the isotopologues of fluoroxene are shown as Supporting Information in Tables S2-S6, and their rotational constants are summarized in Table 3. The isotopic data unambiguously confirm the C_S conformation of the molecule, with all carbons and oxygen skeleton being contained in the C_S plane as observed in the constant value of the planar moment P_c in Table 3, giving the mass extension out of the *c* axis. It may be noted that the A rotational constant of one of the isotopologues ($^{13}C_5$) is slightly larger than that of the parent species due to the proximity of this atom to the *a* principal axis and vibrational effects. A substitution structure (r_s) (arising from Kraitchman's equations)[36] and ground-state effective (r_0) coordinates were calculated from the rotational constants in Tables 2 and 3, assuming C_S symmetry. Both structures are compared to the near-equilibrium (r_e) *ab initio* predictions of fluoroxene in Table 4 (atomic coordinates in Table S7). A visual comparison between predicted (r_e, MP2) and with the different meaning of the r_S (closer to the equilibrium values) and r_0 (vibrational ground state) experimental structures is depicted in Figure 6. Figures S1 to S6 (which provide a 3D interactive view) display the correspondence between the r_S and r_0 structures and the MP2, M06-2X and B3LYP predictions, although we are aware that these quantities must be compared with caution.

After removal of the lines assigned to the isotopologues of fluoroxene, a total of 1650 peaks with a SNR ≥ 3/1 remain unassigned in the spectrum. Attempts to assign these lines to the higher energy conformers of fluoroxene proved unsuccessful. Several molecular species may be the carriers of this spectrum, among them the fluoroxene dimer, fluoroxene-water complexes[37], Van der Waals complexes with the carrier gas[38] or decomposition products. Another aspect that should not be overlooked is that the commercial sample contains 3% of impurities. As we were able to detect transitions due to ^{18}O species (~0.2%), many observed lines will presumably arise from sample impurities.

Discussion

The combination of rotational data and theoretical calculations fully specified the molecular properties of the general anesthetic fluoroxene. A single dominant conformation was observed in the rotational spectrum, with no evidence of higher-energy conformers. We observed that under isolation conditions fluoroxene adopts a *cis-trans* planar conformation of C_S symmetry. This result is consistent with the conclusions of the infrared study of Charles et al.[30] which predicted a planar conformation and the low resolution microwave study by True and Bohn,[31] who proposed a *cis-trans* conformation. The present rotational study discards the observation of any *cis-gauche* conformation suggested previously.[32]

The structural observations can be rationalized based on the PES of Figure 5. Molecular populations in a jet expansion are determined by the global topology of the PES, with the potential barriers between conformations determining whether collisional relaxation is effective in the expansion or individual minima are trapped within their potential wells. In the fluoroxene PES four minima are apparent. However, the most stable *cis-trans* and *cis-gauche* conformations are connected by tiny potential barriers (3.9 kJ mol^{-1}, panel A in Figure 5), thus transferring the population to the global minimum. Similarly, the two *trans-gauche* and *trans-trans* species again plausibly converge in a single conformation because of the low interconversion barrier (2.5 kJ mol^{-1}, panel D in Figure 5). However, the conformational relaxation by a torsion of the vinyl group like *trans-trans* to *cis-trans* or *trans-gauche* to *cis-gauche* exhibits larger barriers (11.1-11.5 in panels B and C of Figure 5). Previous information on collisional relaxation in jet expansions suggested that barriers between 5 to 12 kJ mol^{-1} may prevent conformational isomerization, depending on the complexity and degrees of freedom of the PES. In consequence, and from the potential energy barriers to conformational interconversion, we can state that *cis-gauche* relaxes to *cis-trans* and *trans-trans* to *trans-gauche* upon supersonic expansion. A second fluoroxene conformation could be expected, conformer *trans-gauche*, but very depopulated. However, its small abundance and its small μ_a value make its spectrum difficult to be detected.[39]

The planarity of the *cis-trans* molecular skeleton can be explained in terms of a possible conjugation between the oxygen lone pairs and the vinyl group. This resonance effect is strongly favored in a planar conformation, like the one observed in our experiment. Such planarity was observed in other vinyl ethers such as methyl vinyl ether and was attributed to the same conjugation phenomenon.[40,41] Although the *cis* conformation of the vinyl group in fluoroxene may show larger steric hindrance than the *trans*, it is also the preferred form in several vinyl ethers such as methyl vinyl ether[40,41,42] or ethyl vinyl ether.[43,44] This effect was attributed to the smaller electrostatic repulsion between the lone pair electrons of the oxygen and the π electrons of the double bond in the *cis* configuration.[45]

Besides fluoroxene, other halogenated ethers that also display general anesthetics properties were investigated in the gas phase by rotational spectroscopy. Only one conformer was detected for sevoflurane,[23] whereas two conformers were observed for isoflurane in the gas phase.

The absence of internal rotation hyperfine effects in the spectrum of fluoroxene can be explained due to the large moment of inertia of the CF_3 internal rotor, for which the predicted internal rotation barrier is 19 kJ/mol at MP2/6-311++g(d,p) level.

Furthermore, accurate values of the rotational and centrifugal distortion constants, together with the molecular structure, were determined in the present study for the first time, by analyzing data of the parent species and five isotopologues in natural abundance. Assignments and measurements of the rotational spectra of 5 isotopologues of fluoroxene arising from ^{13}C and ^{18}O substitution in natural abundance with good SNR proves the sensitivity of the CP-FTMW spectrometer. The determined substitution (r_S) and effective (r_0) structures of the molecular skeleton of fluoroxene, despite not directly comparable with the equilibrium theoretical predictions, are in excellent agreement with the MP2 calculation, the discrepancies ranging between 0.0 and 2.2%. There are only two parameters with relative errors greater than 2%: the C_4-C_5 distance (2.0%) and the O_3-C_4-C_5 angle (2.2%) (MP2 predictions compared to r_S). These two parameters involve atoms (in particular, C_4 and C_5) lying close to one of the principal axes, which explains the larger uncertainties for these values.

Finally, the present structural study serves as a basis for future microsolvation and molecular recognition investigations about intermolecular complexes with the aim of shedding light on the structure-activity relationship of this kind of drugs.

ACKNOWLEDGEMENTS

The authors wish to thank the MICINN and MINECO (CTQ-2014-54464-R, CTQ-2012-39132), the Basque Government (IT520-10) and the UPV/EHU (UFI11/23) for funds. E.J.C. and I. U. acknowledges a “Ramón y Cajal” contract and FPU grant from the MICINN. Computational resources of SGIker and laser facilities at the UPV/EHU were used in this work (SGIker). L. S. thanks the University of Bologna for a scholarship to visit the UPV/EHU.

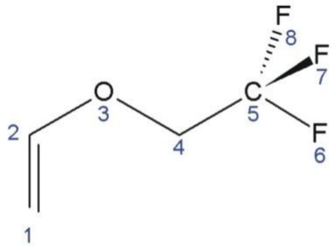

Scheme 1. Structure and atom numbering for the fluoroxene molecule.

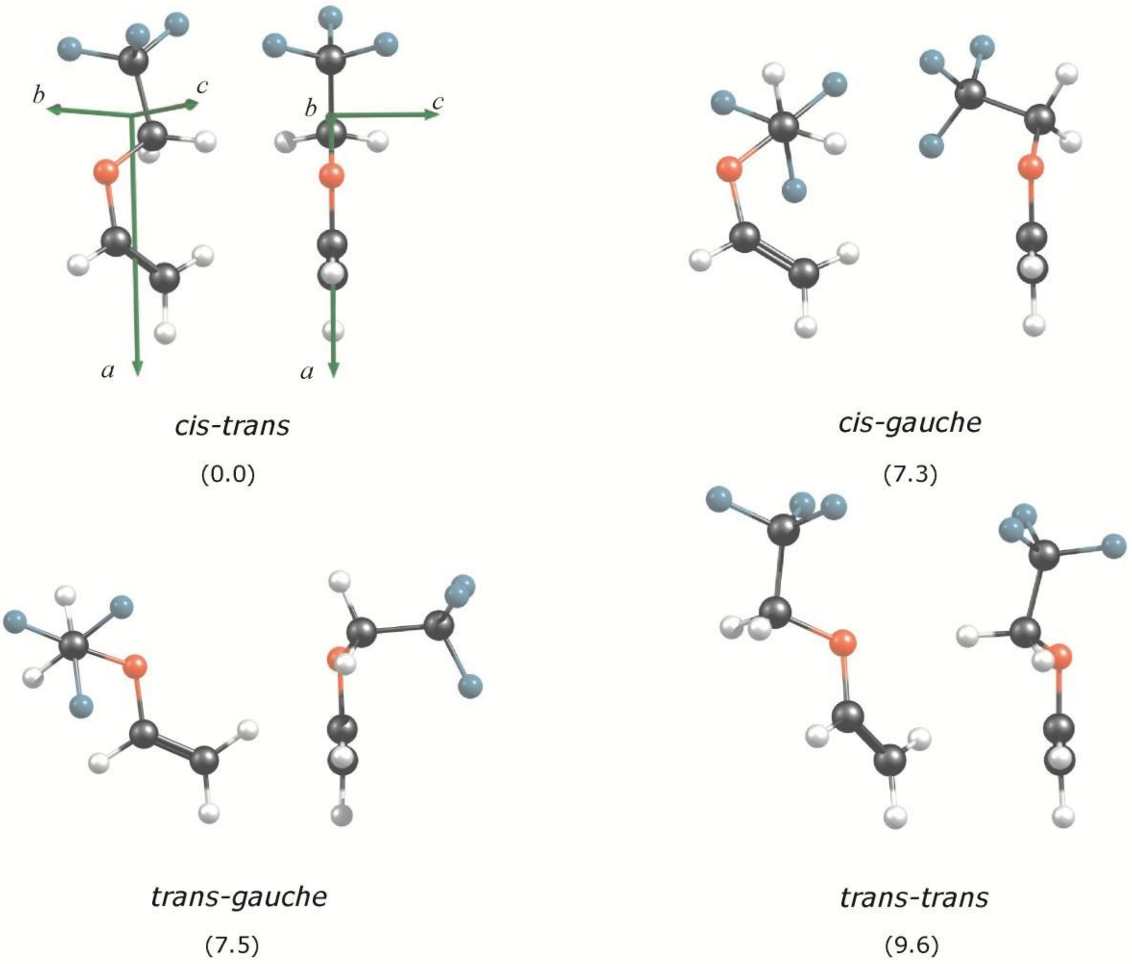

cis-trans
(0.0)

cis-gauche
(7.3)

trans-gauche
(7.5)

trans-trans
(9.6)

Figure 1. Lowest-lying conformers of fluoroxene within an energy window in the 0-20 kJ mol^{-1} range (with relative energies (MP2/6-311++G(d,p)/ZPE corrected) in kJ mol^{-1} shown in brackets), atom labelling and principal inertial axis system (front and side views are displayed). The conformers are named as follows: *conformation vinyl-conformation trifluoroethoxy*.

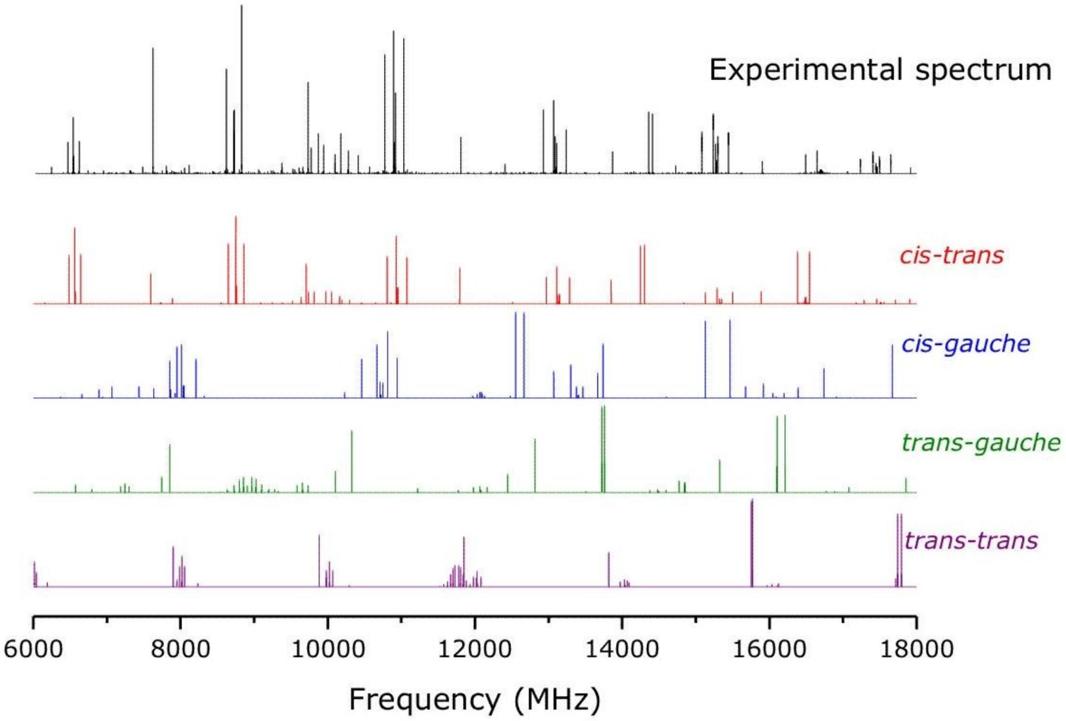

Figure 2. Experimental rotational spectrum of fluoroxene and predicted MP2 spectra for the four lowest-lying conformers.

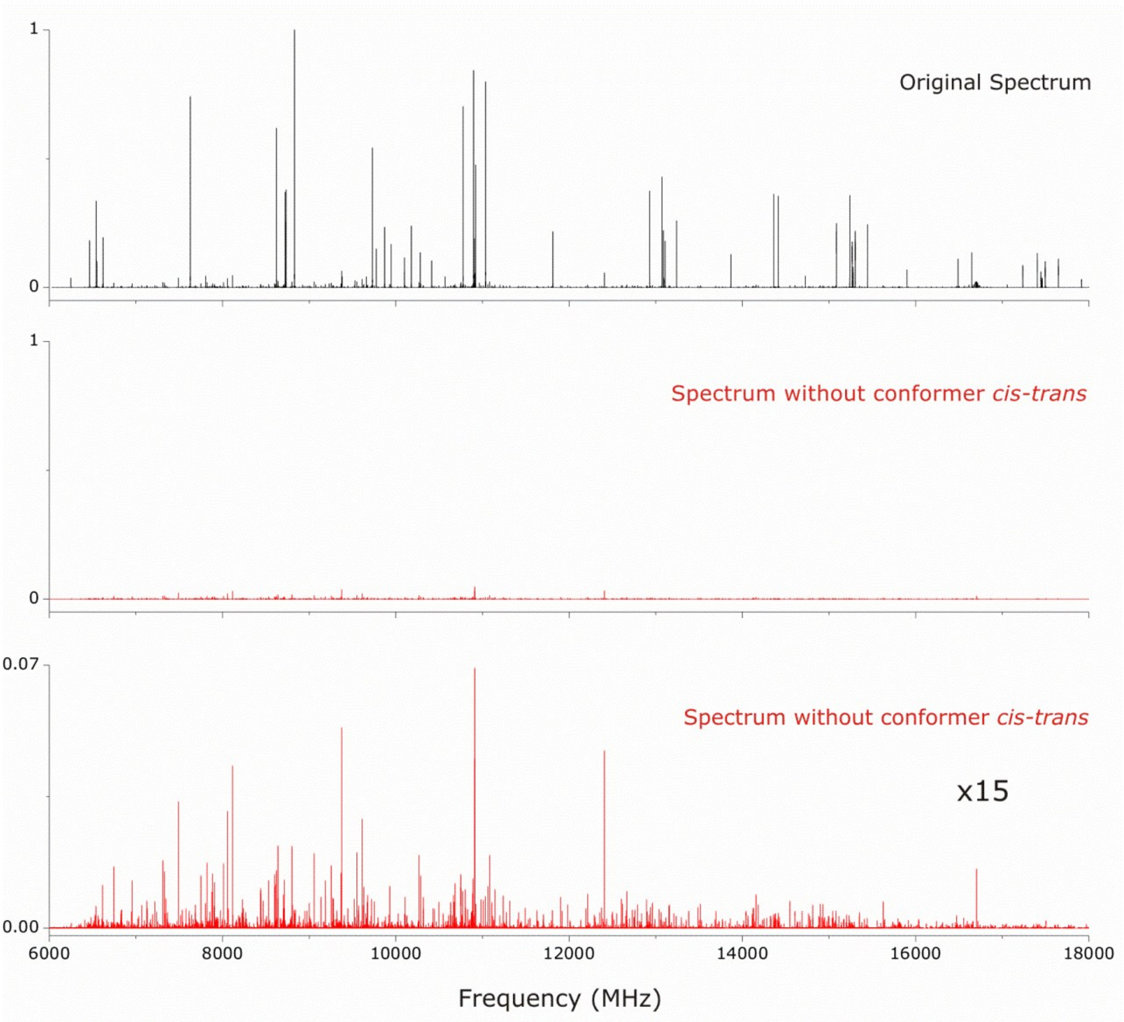

Figure 3. Comparison between the original spectrum of fluoroxene and the result of removing the lines assigned to conformer *cis-trans*, showing that the most intense lines correspond to this conformer. In the normalized spectrum below it can be clearly seen that a large number of weak rotational transitions still remain.

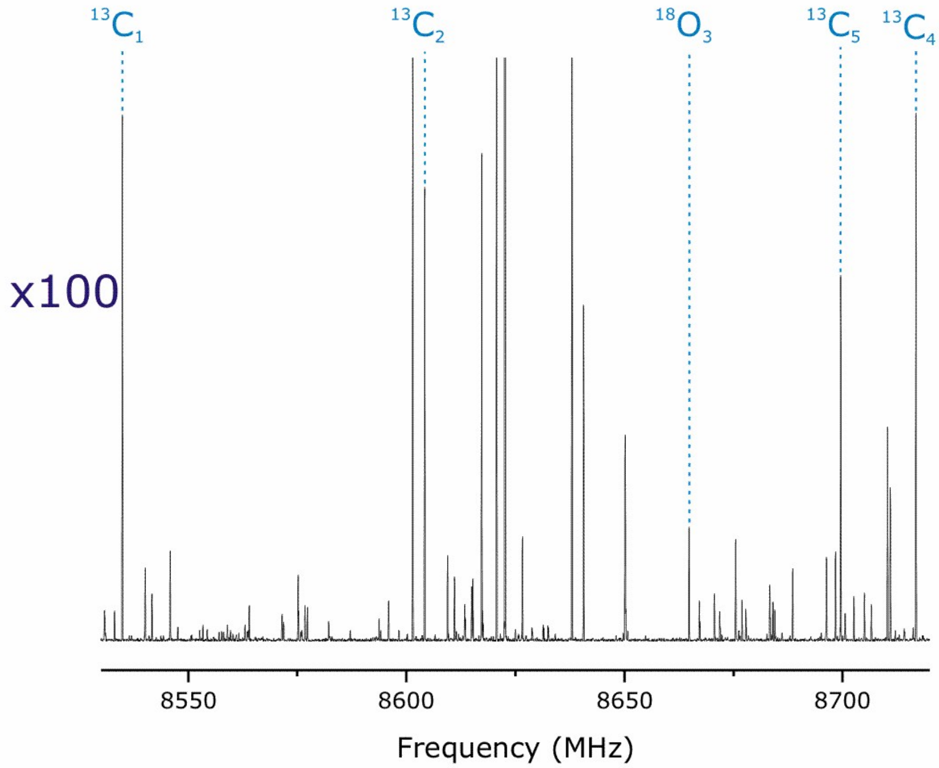

Figure 4. Assignment of the $4_{0,4} \leftarrow 3_{0,3}$ transition for the different isotopologues of fluoroxene.

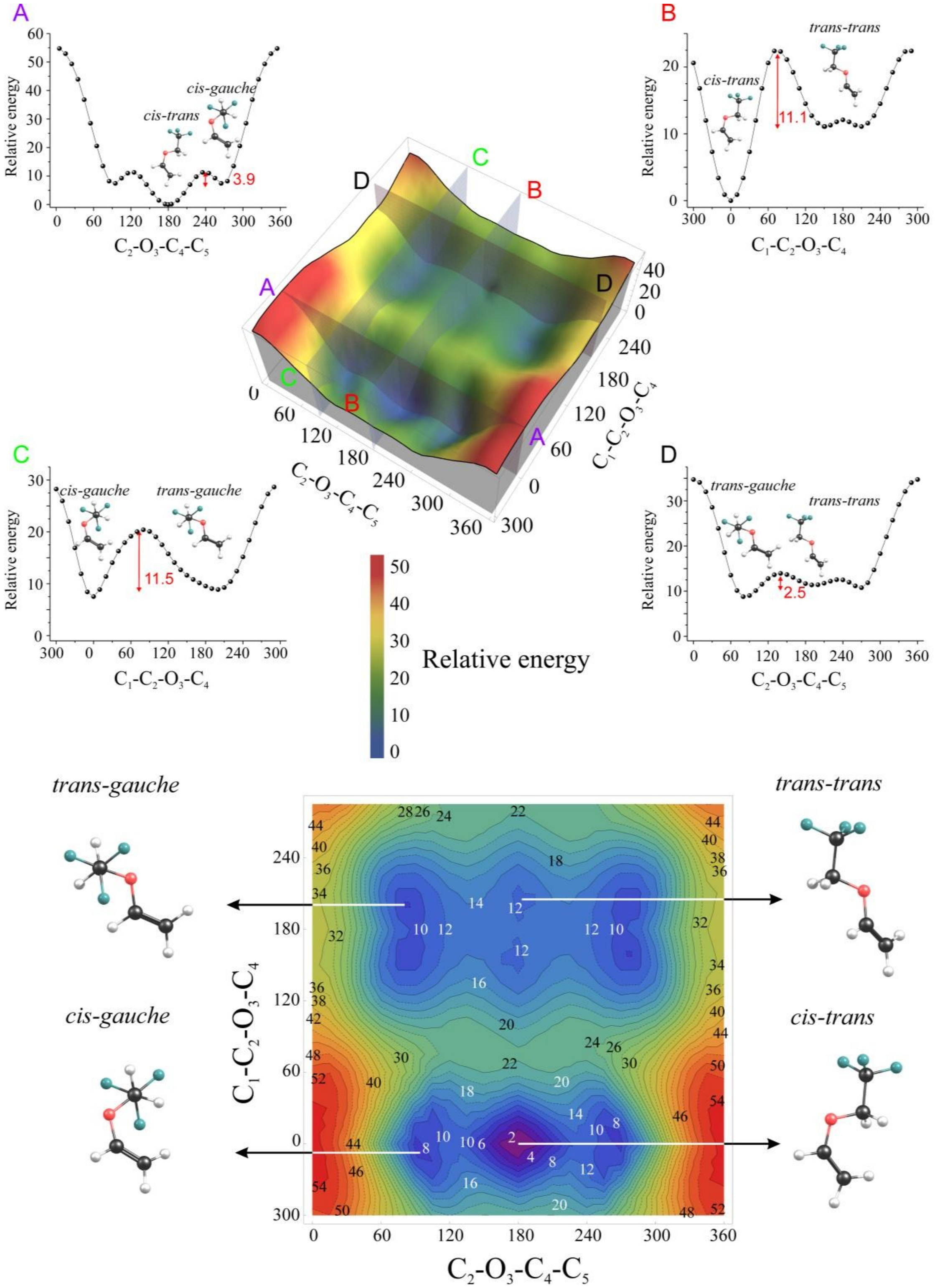

Figure 5. The *ab initio* (MP2/6-311++G(d,p)) PES of fluoroxene shows two wells and four distinct local minima. The independent variables correspond to the torsion angles C_1-C_2-O_3-C_4 and C_2-O_3-C_4-C_5 defined in Scheme 1 (energies in kJmol^{-1}, angles in degrees).

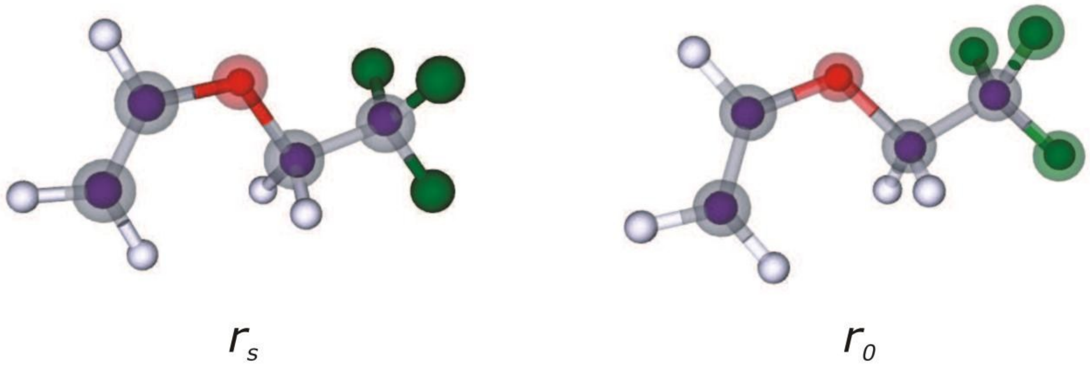

Figure 6. Experimental structures (r_S and r_0) of fluoroxene compared to the *ab initio* structure (MP2/6-311++G(d,p) level). The larger spheres (transparent and/or solid) are the theoretical positions, while the smaller solid spheres represent the experimental structures.

Table 1. Predicted rotational constants, dipole moment components and relative energies of the four lowest lying conformers of fluoroxene at MP2, M06-2X and B3LYP respectively. In all cases the Standard Pople's triple-ζ 6-311++G(d,p) basis set was used.

	Conformer ***cis-trans***	**Conformer** ***cis-gauche***	**Conformer** ***trans-gauche***	**Conformer** ***trans-trans***
A/MHz[a]	4393.5/4455.3/4403.1	3756.0/3781.0/3762.1	4178.4/4275.1/4301.9	4919.7/4961.1/4891.8
B/MHz	1121.3/1122.7/1098.9	1398.7/1414.6/1356.1	1226.0/1220.6/1159.0	1011.0/1016.4/1000.0
C/MHz	1067.5/1070.7/1048.9	1278.6/1292.6/1246.8	1189.4/1186.3/1133.9	994.0/997.8/982.5
D_J/kHz	0.067/0.069/0.068	0.27/0.23/0.35	0.55/0.55/0.45	0.052/0.066/0.060
D_{JK}/kHz	1.1/1.3/1.3	0.49/0.60/0.64	-1.4/-1.6/-1.1	2.0/2.0/2.6
D_K/kHz	-0.25/-0.37/-0.33	0.44/0.27/0.56	6.5/7.3/6.6	-0.80/-0.96/-1.5
d_1/Hz	-3.8/-3.4/-3.8	-37.1/-27.5/-55.1	-74.3/-66.2/-49.8	-0.50/0.65/0.54
d_2/Hz	3.7/4.9/3.6	3.9/3.2/5.7	-0.20/-0.66/0.27	0.96/5.7/1.5
P_c/uÅ	46.2/45.8/46.4	50.3/50.0/50.8	54.1/53.1/53.9	47.1/46.3/47.2
$\|\mu_a\|$/D[b]	2.2/2.3/2.2	1.4/1.5/1.5	0.7/0.7/0.8	1.8/1.8/1.7
$\|\mu_b\|$/D	1.4/1.4/1.4	0.0/0.1/0.1	1.0/1.0/0.9	2.1/2.3/2.2
$\|\mu_c\|$/D	0.0/0.0/0.0	1.5/1.6/1.6	1.7/1.7/1.8	0.9/0,7/0.7
$\|\mu_{tot}\|$/D	2.6/2.7/2.6	2.1/2.2/2.2	2.1/2.1/2.9	2.9/3.0/2.9
$\Delta E+ZPE$/kJ mol^{-1}[c]	0.0/0.0/0.0	7.3/6.9/7.0	7.5/8.1/4.6	9.6/11.3/6.4
ΔG/kJ mol^{-1}[d]	0.0/0.0/0.0	8.0/9.0/7.0	5.9/7.6/2.9	7.2/7.6/3.4

[a] Rotational constants (A, B, C). [b] Electric dipole moment components ($|\mu_\alpha|$, $\alpha=a, b, c$) referred to the principal inertial axis and total electric dipole moment; 1D≈3.336×10^{-30} C m. [c] Electronic energy with inclusion of zero-point correction. [d] Gibbs free-energy at 298 K.

Table 2. Experimental rotational parameters of the most abundant conformation of fluoroxene and comparison with previous studies.

	This work	**Dennison et al.**[32]
A/MHz[a]	4431.82253(27)[d]	4421.2(4.3)
B/MHz	1116.736849(75)	1128.3(19.6)
C/MHz	1065.058889(76)	1053.7(19.6)
D_J/kHz[b]	0.06793(21)	
D_{JK}/kHz	1.0772(13)	
D_K/kHz	-0.1356(40)	
d_1/Hz	-3.612(46)	
d_2/Hz	3.028(14)	
P_c/uÅ	46.037925(36)	
N[c]	190	
σ/kHz	5.8	

[a]Rotational constants (A, B, C). [b]Watson's S-reduction quartic (D_J, D_{JK}, D_K, d_1, d_2) centrifugal distortion constants and planar moment (P_c). [c]Number of transitions (N) and rms deviation of the fit (σ). [d]Standard errors in parentheses in units of the last digit.

Table 3. Experimental rotational parameters of five isotopologues of fluoroxene detected in natural abundance.

	$^{13}C_1$	**$^{13}C_2$**	**$^{13}C_4$**	**$^{13}C_5$**	**$^{18}O_3$**
A/MHz[a]	4412.97690(32)[c]	4423.94792(28)	4421.63911(18)	4432.01619(30)	4399.56060(57)
B/MHz	1092.87428(10)	1101.629349(73)	1116.491526(68)	1113.907802(83)	1110.37107(12)
C/MHz	1042.28334(10)	1050.865804(59)	1064.253774(64)	1062.474364(90)	1057.42050(12)
P_c/uÅ	46.037680(49)	46.038125(32)	46.039474(30)	46.032982(41)	46.039439(59)
N [b]	83	81	67	72	51
σ/kHz	5.8	5.1	3.3	4.8	5.4

[a] Rotational constants (A, B, C) and planar moment (P_c). Centrifugal distortion constants of the minor isotopologues are fixed to the values of the parent species. [b] Number of transitions (N) and rms deviation of the fit (σ). [c] Standard errors in parentheses in units of the last digit.

Table 4. Substitution (r_s), effective (r_0) and calculated (r_e) structures of fluoroxene in the gas phase.

	r_s	r_0	r_e (MP2)
r (C_1-C_2) / Å	1.335(5)[a]	1.343(5)	1.343
r (C_2-O_3) / Å	1.365(3)	1.364(4)	1.362
r (O_3-C_4) / Å	1.432(8)	1.419(5)	1.407
r (C_4-C_5) / Å	1.482(7)	1.508(7)	1.512
r (C_5-F_6) / Å		1.343(12)	1.347
r (C_5-F_7) = r (C_5-F_8) / Å		1.334(3)	1.339
∠ (C_1-C_2-O_3) / deg	127.6(4)	127.2(3)	127.5
∠ (C_2-O_3-C_4) / deg	117.1(5)	116.0(3)	115.0
∠ (O_3-C_4-C_5) / deg	105.1(4)	106.8(4)	107.4
∠ (C_4-C_5-F_6) = / deg		108.8(5)	109.0
∠ (F_6-C_5-F_7) = ∠ (F_6-C_5-F_8) / deg		107.4(4)	107.8
τ_1=τ (C_1-C_2-O_3-C_4) / deg	[180.0][b]	[180.0]	180.0
τ_2=τ (C_2-O_3-C_4-C_5) / deg	[0.0]	[0.0]	0.0

[a] Errors in parentheses in units of the last digit. [b] Values in brackets were fixed in the fitting.

ASSOCIATED CONTENT

Supporting Information.

Table S1. Full list of rotational transitions observed (in MHz) for the parent species of fluoroxene.

J’	K’$_{-1}$	K’$_{+1}$	J’’	K’’$_{-1}$	K’’$_{+1}$	obs.^{a}	o.-c.^{b}
8	1	8	7	2	5	6407.5623	-0.0070
3	1	3	2	1	2	6467.4818	-0.0025
3	0	3	2	0	2	6542.9786	-0.0038
3	2	2	2	2	1	6545.3498	-0.0039
3	2	1	2	2	0	6547.7485	-0.0032
3	1	2	2	1	1	6622.5104	-0.0026
14	1	13	14	0	14	6783.5889	-0.0027
11	2	10	10	3	7	7185.9314	-0.0143
14	3	11	13	4	10	7271.0895	-0.0018
15	1	14	15	0	15	7365.9054	-0.0104
11	2	9	10	3	8	7610.3994	-0.0092
2	1	2	1	0	1	7626.9890	-0.0017
5	0	5	4	1	4	7807.0289	-0.0071
3	3	1	4	2	2	7969.2800	-0.0071
3	3	0	4	2	3	7978.2675	-0.0131
16	1	15	16	0	16	8001.3530	-0.0061
6	4	3	7	3	4	8105.2969	-0.0024
6	4	2	7	3	5	8106.2079	-0.0055
9	1	9	8	2	6	8298.1170	-0.0081
8	1	7	7	2	6	8341.0917	-0.0081
16	2	14	16	1	15	8382.1935	0.0077
14	2	12	14	1	13	8455.1633	-0.0004
19	2	17	19	1	18	8582.2291	0.0106
4	1	4	3	1	3	8622.6110	-0.0049
12	2	10	12	1	11	8650.1564	-0.0156
17	1	16	17	0	17	8688.5664	-0.0028
4	0	4	3	0	3	8721.1732	-0.0023
4	2	3	3	2	2	8726.6590	-0.0050
4	3	1	3	3	0	8728.2853	-0.0018
4	3	2	3	3	1	8728.2853	-0.0018
4	2	2	3	2	1	8732.6499	-0.0056
11	2	9	11	1	10	8780.0529	0.0008
4	1	3	3	1	2	8829.2950	-0.0048
10	2	8	10	1	9	8923.9138	0.0083
9	2	7	9	1	8	9075.9590	-0.0045
8	2	6	8	1	7	9230.5879	-0.0040
18	4	15	17	5	12	9300.8667	-0.0093
7	2	5	7	1	6	9382.4335	-0.0049
18	1	17	18	0	18	9425.1993	-0.0086
15	3	12	14	4	11	9490.7339	-0.0158
6	2	4	6	1	5	9526.5523	-0.0059
5	2	3	5	1	4	9658.5119	0.0003

3	1	3	2	0	2	9731.4828	-0.0025
4	2	2	4	1	3	9774.4321	-0.0017
3	2	1	3	1	2	9871.0754	-0.0026
12	2	10	11	3	9	9911.0441	0.0038
2	2	0	2	1	1	9945.8363	-0.0031
6	0	6	5	1	5	10099.6868	-0.0083
2	2	1	2	1	2	10100.2718	-0.0015
3	2	2	3	1	3	10178.1388	-0.0039
4	2	3	4	1	4	10282.1868	-0.0041
5	4	2	6	3	3	10290.3383	-0.0152
5	4	1	6	3	4	10290.7027	-0.0164
5	2	4	5	1	5	10412.5935	-0.0019
11	6	5	12	5	8	10553.3479	0.0022
11	6	6	12	5	7	10553.3479	0.0050
6	2	5	6	1	6	10569.5582	-0.0045
14	7	7	15	6	10	10683.7291	-0.0070
14	7	8	15	6	9	10683.7291	-0.0070
9	1	8	8	2	7	10744.4276	0.0001
9	1	8	8	2	7	10744.4276	0.0001
7	2	6	7	1	7	10753.3299	0.0127
5	1	5	4	1	4	10777.1580	-0.0054
5	0	5	4	0	4	10896.9776	-0.0016
5	2	4	4	2	3	10907.5616	-0.0063
5	2	3	4	2	2	10919.5277	-0.0083
8	2	7	8	1	8	10964.0827	-0.0073
5	1	4	4	1	3	11035.4497	-0.0085
9	2	8	9	1	9	11202.1070	0.0009
13	2	12	12	3	9	11440.2867	-0.0016
10	2	9	10	1	10	11467.5739	0.0047
11	2	10	11	1	11	11760.6520	0.0042
4	1	4	3	0	3	11811.1152	-0.0035
11	1	11	10	2	8	11927.0634	0.0050
12	2	11	12	1	12	12081.4649	0.0044
13	2	11	12	3	10	12239.8142	0.0049
13	2	12	13	1	13	12430.0655	0.0049
7	5	2	8	4	5	12607.0387	0.0043
7	5	3	8	4	4	12607.0387	0.0043
10	6	4	11	5	7	12738.7377	0.0019
14	2	13	14	1	14	12806.4230	0.0001
6	1	6	5	1	5	12930.9926	-0.0042
6	0	6	5	0	5	13069.8116	-0.0108
6	5	1	5	5	0	13091.8962	0.0048
6	5	2	5	5	1	13091.8962	0.0048
6	4	2	5	4	1	13092.5520	0.0046
6	4	3	5	4	2	13092.5520	0.0046
6	3	4	5	3	3	13093.7807	0.0048

6	3	3	5	3	2	13094.0229	0.0035
6	2	4	5	2	3	13108.8583	-0.0031
10	1	9	9	2	8	13169.6460	0.0029
15	2	14	15	1	15	13210.4370	0.0056
6	1	5	5	1	4	13240.8119	-0.0029
3	2	2	3	0	3	13366.6374	-0.0083
4	2	3	4	0	4	13372.1359	0.0016
5	2	4	5	0	5	13382.7022	-0.0207
6	2	5	6	0	6	13400.8556	-0.0088
8	2	7	8	0	8	13471.7434	0.0030
9	2	8	9	0	9	13531.3167	0.0094
14	2	13	13	3	10	13543.2659	0.0003
16	2	15	16	1	16	13641.8674	-0.0010
12	1	12	11	2	9	13655.5661	0.0005
17	3	15	16	4	12	13795.2119	0.0038
5	1	5	4	0	4	13867.1136	0.0069
17	3	14	16	4	13	13962.4294	0.0043
17	2	16	17	1	17	14100.4103	0.0029
2	2	1	1	1	0	14360.5015	-0.0011
2	2	0	1	1	1	14412.7792	-0.0009
18	2	17	18	1	18	14585.6108	0.0044
14	2	12	13	3	11	14599.2154	-0.0006
8	0	8	7	1	7	14728.4164	0.0114
6	5	1	7	4	4	14790.9718	0.0033
6	5	2	7	4	3	14790.9718	0.0033
19	3	16	19	2	17	14909.8798	-0.0101
9	6	3	10	5	6	14923.4116	-0.0001
12	7	5	13	6	8	15054.9970	0.0014
12	7	6	13	6	7	15054.9970	0.0014
7	1	7	6	1	6	15083.9999	0.0032
19	2	18	19	1	19	15096.9094	0.0032
18	3	15	18	2	16	15170.2551	-0.0016
7	0	7	6	0	6	15239.1699	0.0019
7	2	6	6	2	5	15267.7549	0.0039
7	6	1	6	6	0	15273.6125	-0.0001
7	5	2	6	5	1	15274.2290	0.0015
7	5	3	6	5	2	15274.2290	0.0015
7	4	3	6	4	2	15275.2237	0.0036
7	4	4	6	4	3	15275.2237	0.0036
7	3	5	6	3	4	15277.0580	0.0045
7	3	4	6	3	3	15277.6064	0.0053
7	2	5	6	2	4	15301.0673	0.0022
13	1	13	12	2	10	15320.2480	0.0029
17	3	14	17	2	15	15415.3392	-0.0007
7	1	6	6	1	5	15445.1918	0.0070
11	1	10	10	2	9	15615.7749	0.0018

20	2	19	20	1	20	15633.6343	0.0034
16	3	13	16	2	14	15641.2234	0.0018
15	3	12	15	2	13	15844.9765	-0.0020
6	1	6	5	0	5	15901.1280	0.0037
14	3	11	14	2	12	16024.7405	-0.0004
13	3	10	13	2	11	16179.6936	0.0002
18	3	15	17	4	14	16218.8242	0.0115
12	3	9	12	2	10	16310.0175	0.0001
11	3	8	11	2	9	16416.7789	0.0014
3	2	2	2	1	1	16490.5909	-0.0025
10	3	7	10	2	8	16501.7619	0.0014
9	3	6	9	2	7	16567.2875	0.0031
8	3	5	8	2	6	16616.0035	0.0029
3	2	1	2	1	2	16648.6296	0.0048
7	3	4	7	2	5	16650.7115	0.0075
6	3	3	6	2	4	16674.1728	0.0048
5	3	2	5	2	3	16689.0182	0.0081
4	3	1	4	2	2	16697.6027	0.0110
3	3	0	3	2	1	16701.9529	0.0057
4	3	2	4	2	3	16706.5450	-0.0053
5	3	3	5	2	4	16709.8531	0.0075
6	3	4	6	2	5	16715.6628	0.0055
7	3	5	7	2	6	16724.9637	0.0040
8	3	6	8	2	7	16738.8614	0.0043
9	3	7	9	2	8	16758.5730	0.0036
10	3	8	10	2	9	16785.4168	0.0004
11	3	9	11	2	10	16820.8013	0.0009
12	3	10	12	2	11	16866.1908	0.0035
14	1	14	13	2	11	16916.5343	-0.0016
13	3	11	13	2	12	16923.0896	0.0015
5	5	0	6	4	3	16974.2961	-0.0011
5	5	1	6	4	2	16974.2961	-0.0011
15	2	13	14	3	12	16991.2010	-0.0009
14	3	12	14	2	13	16993.0360	-0.0024
9	0	9	8	1	8	17057.8817	0.0040
15	3	13	15	2	14	17077.5760	-0.0035
8	6	2	9	5	5	17107.4741	-0.0014
8	6	3	9	5	4	17107.4741	-0.0014
16	3	14	16	2	15	17178.2326	-0.0054
8	1	8	7	1	7	17236.0595	0.0043
17	3	15	17	2	16	17296.5017	-0.0052
8	0	8	7	0	7	17404.5415	0.0062
8	2	7	7	2	6	17446.8302	0.0021
8	7	1	7	7	0	17455.2440	-0.0034
8	7	2	7	7	1	17455.2440	-0.0034
8	6	2	7	6	1	17455.8609	-0.0065

8	5	3	7	5	2	17456.7268	-0.0001
8	4	4	7	4	3	17458.1619	-0.0039
8	3	6	7	3	5	17460.7267	0.0012
8	3	5	7	3	4	17461.8209	0.0011
8	2	6	7	2	5	17496.5269	0.0037
19	3	17	19	2	18	17591.5712	-0.0046
8	1	7	7	1	6	17648.3724	0.0026
16	2	15	15	3	12	17685.1910	-0.0023
7	1	7	6	0	6	17915.3044	0.0060
12	1	11	11	2	10	18081.6694	0.0008

[a]Observed frequency; [b]Observed-Calculated

Table S2. Full list of rotational transitions observed (in MHz) for the $^{13}C_1$ monosubstituted species of fluoroxene

J'	K'_{-1}	K'_{+1}	J''	K''_{-1}	K''_{+1}	obs.[a]	o.-c. [b]
3	0	3	2	0	2	6403.1692	-0.0017
3	2	2	2	2	1	6405.4365	-0.0029
3	1	2	2	1	1	6480.9811	-0.0033
2	1	2	1	0	1	7539.8187	0.0001
5	0	5	4	1	4	7564.7591	-0.0090
4	1	4	3	1	3	8438.2871	-0.0010
4	0	4	3	0	3	8534.8757	-0.0041
4	2	3	3	2	2	8540.1310	-0.0006
4	3	1	3	3	0	8541.6851	0.0019
4	3	2	3	3	1	8541.6851	0.0019
4	2	2	3	2	1	8545.8605	-0.0058
4	1	3	3	1	2	8640.6223	-0.0032
8	2	6	8	1	7	9257.6625	-0.0076
6	2	4	6	1	5	9549.4089	0.0118
3	1	3	2	0	2	9599.2919	-0.0038
5	2	3	5	1	4	9679.0858	0.0057
4	2	2	4	1	3	9792.8533	-0.0020
6	0	6	5	1	5	9808.8561	0.0014
3	2	1	3	1	2	9887.6136	-0.0010
2	2	0	2	1	1	9960.8570	-0.0074
2	2	1	2	1	2	10112.0598	-0.0033
3	2	2	3	1	3	10188.2861	0.0000
4	2	3	4	1	4	10290.1271	-0.0024
5	2	4	5	1	5	10417.7661	0.0020
5	1	5	4	1	4	10546.7999	-0.0001
6	2	5	6	1	6	10571.3963	0.0083
5	0	5	4	0	4	10664.2937	-0.0074
5	2	4	4	2	3	10674.4315	-0.0030
5	4	2	4	4	1	10676.8468	-0.0101
5	4	1	4	4	0	10676.8468	-0.0101
5	3	2	4	3	1	10677.6672	-0.0053
5	2	3	4	2	2	10685.8835	-0.0068
5	1	4	4	1	3	10799.6696	0.0039
4	1	4	3	0	3	11634.4106	-0.0023
6	1	6	5	1	5	12654.6302	0.0028
6	0	6	5	0	5	12790.8716	-0.0149
6	2	5	5	2	4	12808.2485	-0.0026
6	4	2	5	4	1	12812.6388	0.0075
6	4	3	5	4	2	12812.6388	0.0075
6	3	4	5	3	3	12813.8139	0.0005
6	3	3	5	3	2	12814.0423	0.0010
6	2	4	5	2	3	12828.2693	0.0134

6	1	5	5	1	4	12957.9404	0.0016
5	1	5	4	0	4	13646.3425	0.0093
2	2	1	1	1	0	14281.1862	-0.0039
2	2	0	1	1	1	14332.3524	-0.0025
7	1	7	6	1	6	14761.6538	-0.0008
7	0	7	6	0	6	14914.1138	-0.0056
7	2	6	6	2	5	14941.4838	-0.0003
7	5	3	6	5	2	14947.6835	0.0141
7	5	2	6	5	1	14947.6835	0.0141
7	4	3	6	4	2	14948.6332	0.0079
7	4	4	6	4	3	14948.6332	0.0079
7	3	5	6	3	4	14950.3921	0.0019
7	3	4	6	3	3	14950.9040	0.0013
7	2	5	6	2	4	14973.3794	-0.0008
7	1	6	6	1	5	15115.2680	-0.0008
6	1	6	5	0	5	15636.6565	-0.0027
2	3	9	12	2	10	16348.1634	-0.0006
3	2	2	2	1	1	16365.7371	0.0071
3	2	1	2	1	2	16520.3769	0.0052
9	3	6	9	2	7	16595.3813	0.0080
9	0	9	8	1	8	16621.1875	-0.0069
8	3	5	8	2	6	16642.0887	0.0010
4	3	1	4	2	2	16720.2539	-0.0017
4	3	2	4	2	3	16728.8143	-0.0165
5	3	3	5	2	4	16731.9779	-0.0054
6	3	4	6	2	5	16737.5425	-0.0031
7	3	5	7	2	6	16746.4581	0.0063
9	3	7	9	2	8	16778.6511	0.0066
8	1	8	7	1	7	16867.7779	-0.0004
8	0	8	7	0	7	17033.5313	-0.0036
8	2	7	7	2	6	17074.0384	0.0011
8	5	3	7	5	2	17083.5090	0.0127
8	5	4	7	5	3	17083.5090	0.0127
8	4	4	7	4	3	17084.8797	0.0037
8	4	5	7	4	4	17084.8797	0.0037
8	3	6	7	3	5	17087.3506	0.0042
8	3	5	7	3	4	17088.3735	0.0030
8	2	6	7	2	5	17121.6287	0.0001
8	1	7	7	1	6	17271.4650	-0.0019
7	1	7	6	0	6	17607.4246	-0.0027
4	2	3	3	1	2	18424.8725	-0.0046

[a] Observed frequency; [b] Observed-Calculated

Table S3. Full list of rotational transitions observed (in MHz) for the $^{13}C_2$ monosubstituted species of fluoroxene

J'	K'_{-1}	K'_{+1}	J''	K''_{-1}	K''_{+1}	obs.[a]	o.-c. [b]
3	1	3	2	1	2	6380.9687	0.0007
3	0	3	2	0	2	6455.1686	-0.0008
3	2	2	2	2	1	6457.4486	-0.0034
3	2	1	2	2	0	6459.7430	-0.0182
3	1	2	2	1	1	6533.2500	-0.0036
2	1	2	1	0	1	7576.5366	-0.0003
5	0	5	4	1	4	7649.8983	-0.0042
4	1	4	3	1	3	8507.2871	0.0010
4	0	4	3	0	3	8604.1924	-0.0023
4	2	3	3	2	2	8609.4768	-0.0021
4	3	1	3	3	0	8611.0438	0.0035
4	3	2	3	3	1	8611.0438	0.0035
4	2	2	3	2	1	8615.2399	-0.0090
4	1	3	3	1	2	8710.3111	-0.0026
9	2	7	9	1	8	9108.9080	-0.0073
8	2	6	8	1	7	9262.2718	-0.0082
7	2	5	7	1	6	9412.4863	-0.0016
3	1	3	2	0	2	9653.0917	-0.0023
5	2	3	5	1	4	9684.8310	0.0011
4	2	2	4	1	3	9798.9603	0.0017
3	2	1	3	1	2	9894.0303	0.0068
6	0	6	5	1	5	9911.6466	-0.0042
2	2	0	2	1	1	9967.5172	0.0013
2	2	1	2	1	2	10119.2309	0.0021
3	2	2	3	1	3	10195.7120	-0.0008
4	2	3	4	1	4	10297.9019	-0.0038
5	2	4	5	1	5	10425.9822	0.0031
6	2	5	6	1	6	10580.1357	0.0037
5	1	5	4	1	4	10633.0432	0.0020
5	0	5	4	0	4	10750.9142	-0.0043
7	2	6	7	1	7	10760.5719	-0.0104
5	2	4	4	2	3	10761.1185	0.0041
5	4	2	4	4	1	10763.5378	-0.0146
5	4	1	4	4	0	10763.5378	-0.0146
5	2	3	4	2	2	10772.6341	-0.0063
5	1	4	4	1	3	10886.7721	0.0030
4	1	4	3	0	3	11705.2100	-0.0007
6	1	6	5	1	5	12758.1133	0.0058
6	0	6	5	0	5	12894.7812	-0.0080
6	2	5	5	2	4	12912.2561	-0.0042
6	5	1	5	5	0	12916.0387	0.0062
6	4	2	5	4	1	12916.6775	0.0092

6	4	3	5	4	2	12916.6775	0.0092
6	3	4	5	3	3	12917.8597	0.0027
6	3	3	5	3	2	12918.0886	0.0017
6	1	5	5	1	4	13062.4598	0.0072
5	1	5	4	0	4	13734.0565	-0.0005
2	2	1	1	1	0	14322.6859	0.0002
2	2	0	1	1	1	14374.0262	-0.0004
8	0	8	7	1	7	14478.4136	0.0058
7	1	7	6	1	6	14882.3704	0.0012
7	0	7	6	0	6	15035.2868	-0.0007
7	2	6	6	2	5	15062.8220	0.0025
7	4	4	6	4	3	15070.0130	0.0074
7	4	3	6	4	2	15070.0130	0.0074
7	3	5	6	3	4	15071.7833	0.0033
7	3	4	6	3	3	15072.3000	0.0031
7	2	5	6	2	4	15094.9102	0.0001
7	1	6	6	1	5	15237.1772	-0.0099
6	1	6	5	0	5	15741.2475	0.0015
3	2	2	2	1	1	16424.3917	0.0012
14	1	14	13	2	11	16565.2264	0.0004
3	2	1	2	1	2	16579.5690	0.0015
7	3	4	7	2	5	16686.5397	-0.0049
5	3	2	5	2	3	16723.4583	-0.0002
4	3	1	4	2	2	16731.7291	0.0028
4	3	2	4	2	3	16740.3442	-0.0098
6	3	4	6	2	5	16749.1247	0.0020
8	3	6	8	2	7	16771.4810	0.0078
9	0	9	8	1	8	16777.0605	-0.0015
9	3	7	9	2	8	16790.4783	0.0075
8	1	8	7	1	7	17005.7212	-0.0008
8	0	8	7	0	7	17171.9448	-0.0012
8	2	7	7	2	6	17212.6994	0.0050
8	4	4	7	4	3	17223.6048	0.0038
8	4	5	7	4	4	17223.6048	0.0038
8	3	6	7	3	5	17226.0824	-0.0020
8	3	5	7	3	4	17227.1207	0.0031
8	2	6	7	2	5	17260.5719	-0.0026
8	1	7	7	1	6	17410.7793	-0.0031
7	1	7	6	0	6	17728.8279	0.0021

[a]Observed frequency; [b]Observed-Calculated

Table S4. Full list of rotational transitions observed (in MHz) for the $^{18}O_3$ monosubstituted species of fluoroxene

J'	K'_{-1}	K'_{+1}	J''	K''_{-1}	K''_{+1}	obs.[a]	o.-c. [b]
3	1	3	2	1	2	6423.5394	-0.0020
3	0	3	2	0	2	6500.8317	0.0004
3	2	2	2	2	1	6503.3425	0.0012
3	2	1	2	2	0	6505.8948	0.0168
3	1	2	2	1	1	6582.3800	-0.0075
2	1	2	1	0	1	7571.8102	-0.0035
5	0	5	4	1	4	7767.5153	-0.0023
4	1	4	3	1	3	8563.9844	-0.0014
4	0	4	3	0	3	8664.8108	-0.0018
4	2	3	3	2	2	8670.6201	-0.0003
4	2	2	3	2	1	8676.9576	-0.0005
5	2	3	5	1	4	9574.5493	0.0073
3	1	3	2	0	2	9660.4038	-0.0045
4	2	2	4	1	3	9692.8760	-0.0002
3	2	1	3	1	2	9791.6662	-0.0096
2	2	0	2	1	1	9868.1784	-0.0072
2	2	1	2	1	2	10026.4035	0.0007
6	0	6	5	1	5	10048.3016	0.0025
4	2	3	4	1	4	10212.8355	-0.0015
5	2	4	5	1	5	10346.4927	-0.0010
5	1	5	4	1	4	10703.8095	-0.0040
5	0	5	4	0	4	10826.2647	-0.0032
5	2	4	4	2	3	10837.4663	-0.0038
5	2	3	4	2	2	10850.1235	-0.0052
5	1	4	4	1	3	10968.4698	0.0067
4	1	4	3	0	3	11723.5594	-0.0035
7	0	7	6	1	6	12344.6289	-0.0123
6	0	6	5	0	5	12984.6032	0.0083
6	2	5	5	2	4	13003.7846	0.0016
6	4	2	5	4	1	13008.6485	0.0076
6	3	3	5	3	2	13010.1999	0.0034
6	2	4	5	2	3	13025.8805	-0.0024
5	1	5	4	0	4	13762.5728	0.0089
2	2	0	1	1	1	14309.6639	0.0006
8	0	8	7	1	7	14653.2266	-0.0040
7	1	7	6	1	6	14981.0825	-0.0004
7	0	7	6	0	6	15139.2296	-0.0001
7	2	6	6	2	5	15169.4533	0.0011
7	3	5	6	3	4	15179.2942	0.0064
7	3	4	6	3	3	15179.8924	0.0066
7	2	5	6	2	4	15204.6765	0.0015
7	1	6	6	1	5	15351.1283	-0.0006

6	1	6	5	0	5	15779.1752	-0.0082
3	2	2	2	1	1	16370.9049	0.0124
3	2	1	2	1	2	16532.9146	-0.0004
8	1	8	7	1	7	17118.2870	-0.0001
8	0	8	7	0	7	17289.6709	-0.0014
8	2	7	7	2	6	17334.3699	-0.0013
8	3	6	7	3	5	17349.0617	0.0028
8	1	7	7	1	6	17540.6813	-0.0005
7	1	7	6	0	6	17775.6639	-0.0075

[a]Observed frequency; [b]Observed-Calculated

Table S5. Full list of rotational transitions observed (in MHz) for the $^{13}C_4$ monosubstituted species of fluoroxene

J’	$K’_{-1}$	$K’_{+1}$	J’’	$K’’_{-1}$	$K’’_{+1}$	obs.[a]	o.-c. [b]
3	1	3	2	1	2	6463.4831	-0.0010
3	0	3	2	0	2	6539.7710	-0.0008
3	2	1	2	2	0	6544.6585	-0.0012
3	1	2	2	1	1	6620.1878	-0.0043
2	1	2	1	0	1	7614.3904	-0.0016
5	0	5	4	1	4	7813.7530	-0.0087
4	1	4	3	1	3	8617.2646	-0.0007
4	0	4	3	0	3	8716.8262	0.0005
4	2	3	3	2	2	8722.4557	0.0049
4	3	1	3	3	0	8724.1119	-0.0031
4	3	2	3	3	1	8724.1119	-0.0031
4	1	3	3	1	2	8826.1888	0.0013
7	2	5	7	1	6	9347.6773	-0.0067
6	2	4	6	1	5	9492.8584	0.0021
5	2	3	5	1	4	9625.9168	-0.0010
3	1	3	2	0	2	9717.0002	-0.0019
4	2	2	4	1	3	9742.9121	0.0016
3	2	1	3	1	2	9840.5087	0.0011
2	2	0	2	1	1	9916.0386	-0.0012
2	2	1	2	1	2	10072.1412	0.0027
6	0	6	5	1	5	10106.3129	-0.0056
3	2	2	3	1	3	10150.8565	-0.0002
4	2	3	4	1	4	10256.0450	0.0029
5	2	4	5	1	5	10387.8762	-0.0001
6	2	5	6	1	6	10546.5699	-0.0002
5	1	5	4	1	4	10770.4503	0.0017
5	0	5	4	0	4	10891.4316	-0.0001
5	2	4	4	2	3	10902.2895	0.0066
5	2	3	4	2	2	10914.5417	-0.0046
5	1	4	4	1	3	11031.5366	-0.0022
4	1	4	3	0	3	11794.4966	0.0008
6	1	6	5	1	5	12922.9020	0.0011
6	0	6	5	0	5	13063.0132	0.0078
6	2	5	5	2	4	13081.6029	0.0082
6	2	4	5	2	3	13103.0074	0.0009
6	1	5	5	1	4	13236.0674	-0.0007
5	1	5	4	0	4	13848.1271	0.0084
2	2	1	1	1	0	14329.1499	0.0026
2	2	0	1	1	1	14381.9981	-0.0013
7	1	7	6	1	6	15074.4994	-0.0005
7	0	7	6	0	6	15230.9994	0.0012
7	2	6	6	2	5	15260.2844	0.0018

7	3	4	6	3	3	15270.3817	-0.0003
7	2	5	6	2	4	15294.4149	0.0016
7	1	6	6	1	5	15439.5881	0.0026
6	1	6	5	0	5	15879.5878	0.0000
3	2	2	2	1	1	16457.6286	0.0007
8	3	5	8	2	6	16565.5689	-0.0013
7	3	4	7	2	5	16601.1083	0.0047
3	2	1	2	1	2	16617.4137	0.0010
6	3	3	6	2	4	16625.1342	-0.0006
5	3	2	5	2	3	16640.3380	-0.0002
3	3	0	3	2	1	16653.5852	-0.0061
4	3	2	4	2	3	16658.3087	-0.0005
5	3	3	5	2	4	16661.6831	-0.0035
6	3	4	6	2	5	16667.6446	0.0025
9	0	9	8	1	8	17064.0736	0.0014
8	1	8	7	1	7	17225.1350	-0.0015
8	0	8	7	0	7	17394.9151	-0.0054
8	2	7	7	2	6	17438.2442	0.0007
8	4	4	7	4	3	17449.8616	-0.0006
8	4	5	7	4	4	17449.8616	-0.0006
8	3	6	7	3	5	17452.4759	-0.0031
8	3	5	7	3	4	17453.6159	0.0001
8	2	6	7	2	5	17489.1502	0.0010
8	1	7	7	1	6	17641.8841	-0.0029
7	1	7	6	0	6	17891.0777	-0.0045

[a] Observed frequency; [b] Observed-Calculated

Table S6. Full list of rotational transitions observed (in MHz) for the $^{13}C_5$ monosubstituted species of fluoroxene

J’	K’$_{-1}$	K’$_{+1}$	J’’	K’’$_{-1}$	K’’$_{+1}$	obs.[a]	o.-c. [b]
3	1	3	2	1	2	6451.6177	0.0034
3	0	3	2	0	2	6526.7651	-0.0013
3	2	2	2	2	1	6529.1088	-0.0042
3	2	1	2	2	0	6531.4843	-0.0020
3	1	2	2	1	1	6605.9071	-0.0023
2	1	2	1	0	1	7619.4274	-0.0035
5	0	5	4	1	4	7776.0458	0.0012
4	1	4	3	1	3	8601.4617	-0.0010
4	0	4	3	0	3	8699.5823	-0.0006
4	2	3	3	2	2	8705.0191	0.0045
4	3	1	3	3	0	8706.6260	0.0056
4	3	2	3	3	1	8706.6260	0.0056
4	2	2	3	2	1	8710.9427	-0.0016
4	1	3	3	1	2	8807.1683	-0.0007
10	2	8	10	1	9	8936.0578	0.0095
7	2	5	7	1	6	9393.7015	-0.0051
3	1	3	2	0	2	9718.8750	-0.0013
4	2	2	4	1	3	9784.2530	-0.0006
3	2	1	3	1	2	9880.4592	-0.0190
2	2	0	2	1	1	9954.9043	0.0029
6	0	6	5	1	5	10062.8572	-0.0095
2	2	1	2	1	2	10108.6079	0.0000
3	2	2	3	1	3	10186.1084	0.0016
4	2	3	4	1	4	10289.6638	0.0052
5	2	4	5	1	5	10419.4420	0.0027
6	2	5	6	1	6	10575.6617	0.0086
5	1	5	4	1	4	10750.7361	0.0029
7	2	6	7	1	7	10758.5144	-0.0085
5	0	5	4	0	4	10870.0370	0.0025
5	2	4	4	2	3	10880.5088	-0.0050
5	4	2	4	4	1	10883.0137	-0.0094
5	4	1	4	4	0	10883.0137	-0.0094
5	2	3	4	2	2	10892.3605	0.0015
5	1	4	4	1	3	11007.8098	0.0030
4	1	4	3	0	3	11793.5721	-0.0006
7	0	7	6	1	6	12365.1883	0.0049
6	1	6	5	1	5	12899.2887	-0.0077
6	0	6	5	0	5	13037.5616	0.0063
6	2	5	5	2	4	13055.5062	-0.0042
6	4	2	5	4	1	13060.0504	0.0055
6	4	3	5	4	2	13060.0504	0.0055
6	3	4	5	3	3	13061.2648	0.0024

6	3	3	5	3	2	13061.5117	0.0096
6	2	4	5	2	3	13076.2001	0.0065
6	1	5	5	1	4	13207.6431	-0.0081
5	1	5	4	0	4	13844.7231	0.0001
2	2	1	1	1	0	14358.4978	-0.0012
2	2	0	1	1	1	14410.5269	0.0010
8	0	8	7	1	7	14679.8818	0.0012
7	1	7	6	1	6	15047.0335	-0.0006
7	0	7	6	0	6	15201.6126	-0.0005
7	2	6	6	2	5	15229.9034	-0.0005
7	2	5	6	2	4	15262.8737	-0.0041
7	1	6	6	1	5	15406.5199	0.0005
3	2	2	2	1	1	16483.4233	0.0023
3	2	1	2	1	2	16640.6954	0.0076
5	3	2	5	2	3	16703.6716	0.0007
4	3	1	4	2	2	16712.1629	-0.0022
4	3	2	4	2	3	16721.0296	-0.0022
6	3	4	6	2	5	16730.0458	0.0012
8	3	6	8	2	7	16753.0071	-0.0012
9	0	9	8	1	8	17003.5568	0.0006
8	1	8	7	1	7	17193.8388	-0.0009
8	0	8	7	0	7	17361.7321	0.0008
8	2	7	7	2	6	17403.5876	-0.0072
8	4	4	7	4	3	17414.8094	-0.0002
8	4	5	7	4	4	17414.8094	-0.0002
8	3	6	7	3	5	17417.3553	0.0040
8	3	5	7	3	4	17418.4289	0.0006
8	2	6	7	2	5	17452.7842	-0.0013
8	1	7	7	1	6	17604.2157	0.0003
7	1	7	6	0	6	17883.4649	0.0009

[a]Observed frequency; [b]Observed-Calculated

Table S7. Cartesian coordinates (Å) of fluoroxene atoms for the different structural determinations

	r_S[a]	r_0	r_e
	a/ b/ c	*a/ b/ c*	*a/ b/ c*
C_1	3.1484(5)[b]/0.710(2)/[0.000][c]	3.152(2)/0.713(3)/[0.000]	3.026/0.659/0.000
C_2	2.4962(6)/-0.456(3)/[0.000]	2.501(2)/-0.461(4)/[0.000]	2.368/-0.512/0.000
O_3	1.1454(13)/-0.654(2)/[0.000]	1.151(3)/-0.655(3)/[0.000]	1.020/-0.705/0.000
C_4	0.316(5)/0.514(3)/[0.000]	0.354(6)/0.519(3)/[0.000]	0.249/0.472/0.000
C_5	-1.0746(14)/0.000(1)/[0.000]	-1.085(5)/0.068(8)/[0.000]	-1.205/0.060/0.000
F_6		-1.878(6)/1.152(3)/ [0.000]	-1.974/1.167/0.000
F_7		-1.390(6)/-0.650(3)/1.081(3)	-1.523/-0.660/1.083
F_8		-1.390(6)/-0.650(3)/-1.081(3)	-1.523/-0.660/-1.083

[a] Substitution (r_S), effective (r_0) and *ab initio* (MP2/6-311++G(d,p)) equilibrium (r_e) structures [b] Standard errors in parentheses in units of the last digit. [c] Values in brackets were fixed in the fitting.

References

---

[1] N. P. Franks, W. R. Lieb, *Nature* **1994**, *367*, 607-614.

[2] P.-L. Chau, *Br. J. Pharmacol*, **2010**, *161*, 288-307.

[3] I. Leon, E. J. Cocinero, J. Millán, A. M. Rijs, S. Jaeqx, A. Lesarri, F. Castaño, J. A. Fernández, *Phys. Chem. Chem. Phys.*, **2012**, *14*, 4398-4409.

[4] E. Aguado, A. Longarte, E. Alejandro, J. A. Fernández, F. Castaño, *J. Phys. Chem. A* **2006**, *110*, 6010-6015.

[5] I. León, J. Millán, E.J. Cocinero, A. Lesarri, J.A. Fernández, *Angew. Chem. Int. Ed.*, **2013,** *52*, 7772-7775.

[6] E. Aguado, I. Leon, J. Millan, E. J. Cocinero, S. Jaeqx, A. M. Rijs, A. Lesarri, J. A. Fernandez, *J. Phys. Chem. B* **2013**, *117*, 13472-13480.

[7] E. Gloaguen, B. de Courcy, J.-P. Piquemal, J. Pilmé, O. Parisel, R. Pollet, H. S. Biswal, F. Piuzzi, B. Tardivel, M. Broquier, M. Mons, *J. Am. Chem. Soc.* **2010**, *132*, 11860-11863.

[8] J. A. Stearns, O. V. Boyarkin, T. H. Rizzo, *J. Am. Chem. Soc.* **2007**, *129*, 13820–13821.

[9] E. J. Cocinero, E. Stanca-Kaposta, D. P. Gamblin, B. G. Davis, J. P. Simons, *J. Am. Chem. Soc.* **2009**, *131*, 1282-1287.

[10] I. Compagnon, J. Oomens, G. Meijer, G. von Helden, *J. Am. Chem. Soc.* **2006**, *128*, 3592-3597.

[11] E. J. Cocinero, E. C. Stanca-Kaposta, E. M. Scanlan, D. P. Gamblin, B. G. Davis, J. P. Simons, *Chem. Eur. J.*, **2008**, *14*, 8947-8955.

[12] E. J. Cocinero, P. Çarçabal, T. D. Vaden, J. P. Simons, B. G. Davis, *Nature* **2011**, *469*, 76-79.

[13] E. J. Cocinero, D. P. Gamblin, B. G. Davis, J. P. Simons, *J. Am. Chem. Soc.* **2009**, *131*, 11117-11123.

[14] E. J. Cocinero, E. C. Stanca-Kaposta, M. Dethlefsen, B. Liu, D. Gamblin, B. Davis, J. Simons, *Chem. Eur. J.* **2009**, *15*, 13427-13434.

[15] D. Sivanesan, I. Sumathi, W. J. Welsh, *Chem. Phys. Lett.* **2003**, *367*, 351-360.

[16] E. Nir, C. Janzen, P. Imhof, K. Kleinermanns, M. S. de Vries, *Phys. Chem. Chem. Phys.* **2002**, *4*, 732-739.

[17] E. Nir, K. Kleinermanns, M. S. de Vries, *Nature* **2000**, *408*, 949-951.

[18] E. J. Cocinero, A. Lesarri, P. Écija, F. J. Basterretxea, J.-U. Grabow, J. A. Fernández, F. Castaño, *Angew. Chem. Int. Ed.* **2012**, *51*, 3119-3124.

[19] J. L. Alonso, V. Vaquero, I. Peña, J. C. López, S. Mata, W. Caminati, *Angew. Chem. Int. Ed*. **2013**, *52*, 2331-2334.

[20] D. Banser, M. Schnell, J.-U. Grabow, E. J. Cocinero, A. Lesarri, J. L. Alonso, *Angew. Chem. Int. Ed.* **2005**, *44*, 6311-6315.

[21] D. Patterson, M. Schell, J. M. Doyle, *Nature* **2013**, *497*, 475-477.

[22] T. J. Balle, W. H. Flygare, *Rev. Sci. Instrum.* **1981**, *52*, 33-45.

[23] A. Lesarri, A. Vega-Toribio, R.D. Suenram, D.J. Brugh, J.-U. Grabow, *Phys. Chem. Chem. Phys.* **2010**, *12*, 9624-9631.

[24] A. Lesarri, A. Vega-Toribio, R.D. Suenram, D.J. Brugh, D. Nori-Shargh, J.E. Boggs, J.-U. Grabow, *Phys. Chem. Chem. Phys.* **2011**, *13*, 6610-6618.

[25] Q. Gou, G. Feng, L. Evangelisti, M. Vallejo-López, L. Spada, A. Lesarri, E.J. Cocinero, W. Caminati, *Chem. Eur. J.* **2014**, *20*, 1980-1984.

[26] G.G. Brown, B.C. Dian, K.O. Douglass, S.M. Geyer, S.T. Shipman, B.H. Pate, *Rev. Sci. Instrum.* **2008**, *79*, 053103/1-053103/13.

[27] A. Lesarri, S. T. Shipman, J. L. Neill, G. G. Brown, R. D. Suenram, L. Kang, W. Caminati, B. H. Pate, *J. Am. Chem. Soc.* **2010**, *132*, 13417-13424.

[28] N. A. Seifert, C. Pérez, J. L. Neill, B. H. Pate, M. Vallejo-López, A. Lesarri, E. J. Cocinero, F. Castaño, *Phys. Chem. Chem. Phys.* **2015**, *17*, 18282-18287.

[29] N.A. Seifert, D.P. Zaleski, C. Pérez, J.L. Neill, B.H. Pate, M. Vallejo-López, A. Lesarri, E.J. Cocinero, F. Castaño, I. Kleiner, *Angew. Chem. Int. Ed.* **2014**, *53*, 3210-3213.

[30] S. W. Charles, F. C. Cullen, N. L. Owen, *J. Chem. Soc. Faraday Trans. 2* **1974**, *70*, 483-491.

[31] N. S. True, R. K. Bohn, *J. Chem. Phys.* **1975**, *62*, 3951-3954.

[32] F. T. Dennison, C. W. Gillies, S. J. Borchert, *J. Chem. Phys.* **1981**, *75, 3238-3251.*

[33] T.A. Halgren, *J. Comput. Chem.* **1999**, *20*, 730-748.

[34] M. J. Frisch, G. W. Trucks, H. B. Schlegel, G. E. Scuseria, M. A. Robb, J. R. Cheeseman, G. Scalmani, V. Barone, B. Mennucci, G. A. Petersson, H. Nakatsuji, M. Caricato, X. Li, H. P. Hratchian, A. F. Izmaylov, J. Bloino, G. Zheng, J. L. Sonnenberg, M. Hada, M. Ehara, K. Toyota, R. Fukuda, J. Hasegawa, M. Ishida, T. Nakajima, Y. Honda, O. Kitao, H. Nakai, T. Vreven, J. A. Montgomery, Jr., J. E. Peralta, F. Ogliaro, M. Bearpark, J. J. Heyd, E. Brothers, K. N. Kudin,

---

V. N. Staroverov, R. Kobayashi, J. Normand, K. Raghavachari, A. Rendell, J. C. Burant, S. S. Iyengar, J. Tomasi, M. Cossi, N. Rega, J. M. Millam, M. Klene, J. E. Knox, J. B. Cross, V. Bakken, C. Adamo, J. Jaramillo, R. Gomperts, R. E. Stratmann, O. Yazyev, A. J. Austin, R. Cammi, C. Pomelli, J. W. Ochterski, R. L. Martin, K. Morokuma, V. G. Zakrzewski, G. A. Voth, P. Salvador, J. J. Dannenberg, S. Dapprich, A. D. Daniels, Ö. Farkas, J. B. Foresman, J. V. Ortiz, J. Cioslowski, D. J. Fox, Gaussian, Inc., Wallingford CT, **2009**.

[35] J. K. Watson in *Vibrational Spectra and Structure, Vol. 6*, (Ed.: J. R. Durig), Elsevier, Amsterdam, **1977**, pp. 1 – 89.
[36] H. D. Rudolph, in *Advances in Molecular Structure Research*, *Vol. 1* (Eds.: M. Hargittai, I. Hargittai), JAI Press, Greenwich-Connecticut, **1995**, pp. 63-114.
[37] C. Pérez, M. T. Muckle, D. P. Zaleski, N. A. Seifert, B. Temelso, G. C. Shields, Z. Kisiel, B. H. Pate, *Science* **2012**, *336*, 897-901.
[38] A. Dell'Erba, S. Melandri, A. Millemaggi, W. Caminati, P. G. Favero, *J. Chem. Phys.* **2000**, *112*, 2204-2209.
[39] T. Emilsson, T. C. Germann, H. S. Gutowsky, *J. Chem. Phys*. **1992**, *96*, 8830-8839.
[40] N. L. Owen, N. Sheppard, *Trans. Faraday Soc.* **1964**, *60*, 634-645.
[41] J. R. Durig, D. A. C. Compton, *J. Chem. Phys.* **1978**, *69*, 2028-2035.
[42] A. C. Fantoni, W. Caminati, R. Meyer, *J. Chem. Phys*. **1987**, *86*, 1848-1857.
[43] M. Hayashi, N. Inada, *J. Mol. Spectrosc.* **1994**, *165*, 195-204.
[44] N. L. Owen, G. O. Sorensen, *J. Phys. Chem*. **1979**, *83*, 1483-1488.
[45] J. Liu, S. Niwayama, Y. You, K. N. Houk, *J. Org. Chem.* **1998**, *63*, 1064-1073.